JOURNAL OF AGRICULTURAL AND FOOD CHEMISTRY

Article

pubs.acs.org/JAFC

Revealing the Structural Inhomogeneity of Lignins from Sweet Sorghum Stem by Successive Alkali Extractions

Shao-Long Sun,[†] Jia-Long Wen,[†] Ming-Guo Ma,[†] Ming-Fei Li,[†] and Run-Cang Sun*[,†,‡]

[†]Beijing Key Laboratory of Lignocellulosic Chemistry, Beijing Forestry University, Beijing, 100083, China

[‡]State Key Laboratory of Pulp and Paper Engineering, South China University of Technology, Guangzhou, 510640, China

ABSTRACT: To investigate the inhomogeneity of the lignin from sweet sorghum stem, successive alkali treatments were applied to extract lignin fragments in the present study. The successive treatments released 80.3% of the original lignin from the sorghum stem. The chemical structural inhomogeneity of the isolated lignins was comparatively and comprehensively investigated by UV, FT-IR, and NMR spectra. The lignins were found to be predominantly composed of *β*-*O*-4′ aryl ether linkages, together with minor amounts of *β*-*β*′, *β*-5′, *β*-1′, and *α*,*β*-diaryl ether linkages. In addition, hydroxycinnamic acid (mainly *p*-coumaric acid), which was found to be attached to lignin, was released and co-precipitated in the lignin fractions isolated in the initial extracting steps, whereas hydroxycinnamic acids (*p*-coumaric and ferulic acids) were not detected in the subsequently extracted lignin fractions. Moreover, the high proportion of carbon−carbon structures was potentially related to the high amounts of guaiacyl units in the lignin investigated. Thermogravimetric analysis revealed that the higher molecular weights of lignins resulted in relatively higher thermal stability, and the higher content of C−C structures in the lignin probably led to a higher "char residue". These findings suggested that the lignin fractions extracted from sweet sorghum stem by successive alkali extractions had inhomogeneous features in both chemical composition and structure.

KEYWORDS: *sweet sorghum stem, lignin, structural inhomogeneity, 2D-HSQC*

INTRODUCTION

Lignin is one of the most abundant natural phenolic polymers. In general, lignin is an amorphous, tridimensional network inside the cell walls and plays an important role in defense and water transport in vascular terrestrial plants. It is composed of both ether (*β*-*O*-4′, *a*-*O*-4′, and 4-*O*-5′) and C−C (*β*-*β*′, *β*-5′, and *β*-1′) interunit linkages mediated by laccases and/or peroxidases.[1] There are about 20 different types of bonds present within the lignin. Lignin is associated with the hemicellulosic polysaccharides and it is usually derived from three hydroxycinnamyl alcohols (the monolignols: coniferyl, sinapyl, and *p*-coumaryl alcohols), each of which leads to a corresponding type of lignin unit named guaiacyl (G), syringyl (S), and *p*-hydroxyphenyl (H), respectively.[2,3] Up to now, several applications for the lignins from lignocellulosic biomass have been considered, such as a phenol substitute in the formulation of phenol-formaldehyde resins for board manufacture.[4] Chemical modification of lignin used in the preparation of polyurethanes, epoxies, acrylates, composites, and polymer blends has also received a great deal of attention.[5] In addition, lignin may be a potential antioxidant of food oils and fats, which can be used as a food preservative, preventing the loss of food flavor, color, and active vitamin content.[6−8] Nevertheless, a large obstacle for the utilization of lignins in certain application areas, such as synthetic polymers, is the heterogeneity of these lignins and the lack of effective methods for separation of the lignins with a high purity and activity. Better knowledge is required for the separation and structural characterization of lignin if it is to be used optimally. In recent years, successive isolation has been reported to extract lignin from oil palm EFB fiber,[9] bamboo (*Neosinocalamus affinis*),[10] and *Caragana sinica*.[11] However, the inhomogeneous features of lignin have not been thoroughly investigated.

Sweet sorghum is a C4 crop in the Gramineae, belonging to the genus *Sorghum bicolor* L. *Moench*, which also includes grain and fiber sorghum, and is characterized by a high photosynthesis.[12] So far, sweet sorghum in China is mainly used for forage grass and feed and alcohol production.[13] These applications mainly focus on the value-added application of cellulose, such as papermaking and bioethanol production.[14] As known, lignocellulosic biomass (LCB) is a heterogeneous complex of carbohydrates (cellulose and hemicelluloses) and lignin. As the predominant component of LCB, cellulose has been extensively investigated for a hundred years due to its homogeneity.[15] By comparison, lignin has attracted less attention due to its complex structures.[16] As a promising energy plant, scarce information is available on the successive fractionation and inhomogeneous structural and molecular features of sweet sorghum lignin. Therefore, to maximize the utilization of sweet sorghum stem lignin, it is necessary to broaden the knowledge on this aspect.

The aim of the present study is to investigate the inhomogeneity of the lignins from sweet sorghum stem, which are obtained by successive extractions with water, gradual concentrations of KOH, and alkaline ethanol solution. The effects of the successive extractions on the lignin features were evaluated by their yields, associated sugars, and molecular weights. Meanwhile, the structural inhomogeneity of the lignin

Received: February 20, 2013
Revised: April 13, 2013
Accepted: April 14, 2013
Published: April 15, 2013

fractions was comparatively and comprehensively investigated by Fourier transform infrared (FT-IR), ultraviolet/visible (UV), ^{1}H and ^{13}C nuclear magnetic resonance (NMR), and heteronuclear single quantum coherence (HSQC) spectroscopy. Furthermore, to reveal the relationship between structural features (intercoupling bonds, β-O-4′, C−C, etc.) and thermal properties, thermogravimetric analysis (TGA) was also implemented.

MATERIALS AND METHODS

Materials. Sweet sorghum stem was obtained from the experimental farm of the North-Western University of Agricultural and Forest Sciences and Technology (Yangling, P. R. China). The dried raw material was cut into small pieces and then ground and sieved to a 20−40 mesh powder. The dried powder was extracted with 2:1 (v/v) toluene−ethanol in a Soxhlet apparatus for 6 h and then dried in an oven at 60 °C for 16 h before use. The composition (%, w/w) of the dried, dewaxed material was cellulose 42.3%, hemicelluloses 21.8%, and lignin 18.0% (acid-insoluble lignin 15.8% and acid-soluble lignin 2.2%), which was determined by the National Renewable Energy Laboratory's (NREL) standard analytical procedure.[17] All chemicals used were of analytical grade.

Extraction and Purification of Lignin Fractions. The scheme for successive extractions of lignin fractions with dewaxed samples is illustrated in Figure 1. The dewaxed powder was first extracted with water at 90 °C for 3 h with a solid to liquid ratio of 1:20 (g/mL) to obtain water-extractable hemicelluloses. Then the insoluble residue was successively treated with 0.3, 0.6, 1.0, and 1.5% KOH aqueous solutions and 60% ethanol containing 2.5% KOH at 75 °C for 3 h under a solid to liquid ratio of 1:20 (g/mL). The five alkali-extractable filtrates were neutralized to pH 5.5 with acetic acid and evaporated to about 30 mL at reduced pressure. Subsequently, each concentrated solution was poured into three volumes of 95% ethanol with vigorous stirring, and a hemicellulosic pellet was recovered by filtering, washing with 70% aqueous ethanol, and freeze-drying. Then each filtrate was concentrated to about 30 mL, and the pH was adjusted to 1.5−2.0 with 6 M HCl. The lignin fractions were obtained by centrifugation and freeze-drying. All lignin samples were stored in a desiccator for further characterization. The acid-insoluble lignin fractions extracted with 0.3, 0.6, 1.0, and 1.5% KOH aqueous solutions and 60% ethanol containing 2.5% KOH at 75 °C for 3 h were labeled as $L_{0.3}$, $L_{0.6}$, $L_{1.0}$, $L_{1.5}$, and $L_{2.5}$, respectively. All experiments were performed in duplicate. The relative standard deviation, determined by dividing the standard deviation by the mean value, was observed to be lower than 5.0%.

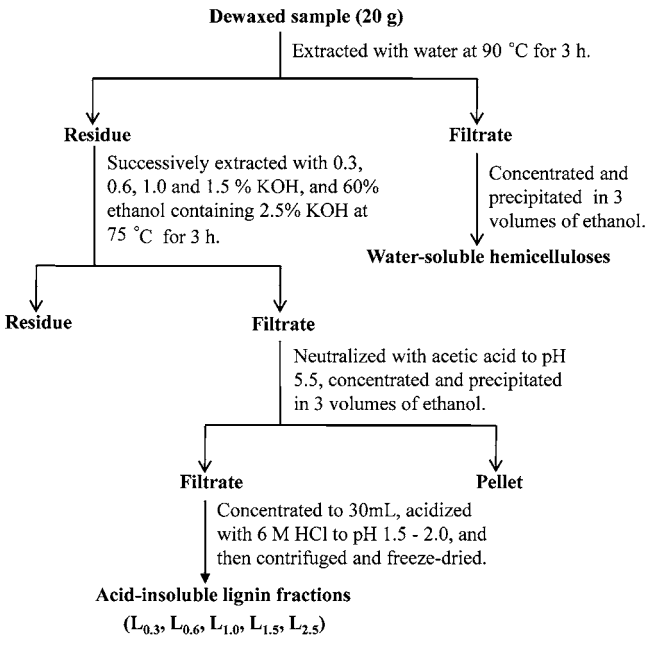

Figure 1. Scheme for successive isolations of lignin fractions from sweet sorghum stem.

Structural Characterization of Lignin Fractions. *Associated Polysaccharides Analysis.* The hemicellulosic polymers associated with the lignin samples were determined by high -performance anion exchange chromatography (HPAEC). The neutral sugars and uronic acids in the fractions (4−6 mg) were liberated by hydrolysis with 1.475 mL of 6% dilute sulfuric acid (H_2SO_4) at 105 °C for 2.5 h. After acid hydrolysis, the samples were diluted 50-fold, and the filtrate containing the liberated neutral sugars was analyzed by an HPAEC system (Dionex ISC 3000) with an amperometric detector, an AS50 autosample, a Carbopac PA-20 column (4 × 250 mm, Dionex), and a PA-20 guard column (3 × 30 mm, Dionex). The sugars were separated in 18 mM NaOH (carbonate free and purged with nitrogen) with postcolumn addition of 0.3 M NaOH at a rate of 0.5 mL/min. Run time was 45 min, followed by 10 min elution with 0.2 M NaOH to wash the column and then a 15 min elution with 18 mM NaOH to re-equilibrate the column. Calibration was performed with standard solution of L-rhamnose, L-arabinose, D-galactose, D-glucose, D-xylose, D-mannose, glucuronic acid, and galacturonic acid. The measurements were conducted in triplicate, and the relative standard deviation was found to be below 3.0%.

GPC Analyses. The molecular weights of the lignin samples were determined by gel permeation chromatography (GPC, Agilent 1200, USA) with a refraction index detector on a PL-gel 10 μm mixed-B 7.5 mm i.d. column, calibrated with polystyrene standards (peaks' average molecular weights of 1320, 9200, 66 000, 435 500, Polymer Laboratories Ltd.). The samples were acetylated with acetic anhydride according to Pan et al., before determination of molecular weights.[8] Briefly, lignin samples were added to mixtures of pyridine−acetic anhydride (1:1, v/v) for 24 h under a nitrogen atmosphere in the dark. At this point, the acetylated lignin samples were recovered by precipitation with acid water (pH 2.0). Then they were washed thoroughly with diethyl ether and dried. A 4 mg amount of acetylated sample was dissolved in 2 mL of tetrahydrofuran (THF), and 20 μL of solution was injected. The column was operated at ambient temperature and eluted with THF at a flow rate of 1.0 mL/min. The measurements were conducted in triplicate, and the relative standard deviation was below 5.0%.

FT-IR Analyses. FT-IR measurements were performed on a Thermo Scientific Nicolet iN10 FT-IR microscope (Thermo Nicolet Corporation, Madison, WI, USA) equipped with a liquid nitrogen cooled MCT detector. The dried samples were ground and pelletized with BaF_2, and the spectra were recorded in the range 4000−800 cm^{-1} at 4 cm^{-1} resolution with 128 scans.

UV Spectral Analyses. UV spectra were obtained on an ultraviolet/visible spectrophotometer (Tec Comp, UV 2300). A 5 mg sample was dissolved in 10 mL of dimethyl sulfoxide (DMSO). A 1 mL aliquot was diluted to 10 mL with DMSO, and the absorbance between 260 and 400 nm was measured.

NMR Spectra of the Lignin Fractions. The solution-state NMR spectra of the lignin samples were recorded on a 400 MHz NMR spectrometer (AVIII 400, Bruker, Germany) at 25 °C. The ^{1}H NMR spectra were obtained at 400 MHz using 10 mg of lignin in 0.5 mL of dimethylsulfoxide-d_6 (DMSO-d_6). The chemical shifts of ^{1}H NMR spectra were calibrated with reference to DMSO, used as an internal standard, at 2.49 ppm. The acquisition time was 3.9 s, and the relaxation time was 1.0 s. The ^{13}C NMR spectra were obtained on a Bruker spectrometer at 100 MHz. The acid-insoluble lignin sample (80 mg) was dissolved in 0.5 mL of DMSO-d_6, and the spectra were recorded at 25 °C after 30 000 scans. A 30° pulse flipping angle, a 9.2 μs pulse width, a 1.36 s acquisition time, and a 1.89 s relaxation delay time were used. For heteronuclear single quantum correlation (HSQC) spectra, the data were acquired by using a 20 mg sample in 0.5 mL of DMSO-d_6. The spectral widths were 2200 and 15 400 Hz for the ^{1}H- and ^{13}C-dimensions, respectively. The number of collected

dx.doi.org/10.1021/jf400824p | J. Agric. Food Chem. 2013, 61, 4226−4235

complex points was 1024 for the ^{1}H-dimension with a recycle delay of 1.5 s. The number of transients was 128, and 256 time increments were recorded in the ^{13}C-dimension. The $^{1}J_{C-H}$ was set to 146 Hz. Prior to Fourier transform the data matrices were zero filled up to 1024 points in the ^{13}C-dimension.

Thermogravimetric Analysis. Thermal behavior of the lignin samples was studied by using thermogravimetric and differential thermogravimetric analysis on a simultaneous thermal analyzer (TGA Q500, USA). About 8−10 mg of samples was heated in a platinum crucible from room temperature to 600 °C at a heating rate of 20 °C/min under a nitrogen atmosphere.

RESULTS AND DISCUSSION

Fractional Yields and Contents of Carbohydrates. The yields of the lignin fractions from sweet sorghum stem are given in Table 1. As can be seen, the yields of lignin were 0.8, 5.2, 2.3, 2.4, and 2.0% (% dried, dewaxed material), corresponding to a release of 5.1, 32.9, 14.5, 14.9, and 12.9% of the original lignin (acid-insoluble lignin), respectively, by sequential extractions with 0.3, 0.6, 1.0, and 1.5% KOH aqueous solutions and 60% ethanol containing 2.5% KOH at 75 °C for 3 h. Taken together, a total yield of the five lignin fractions accounted for 12.7% (% dried, dewaxed material), corresponding to 80.3% of acid-insoluble lignin in the cell walls. Evidently, the highest yield of the five lignin samples was obtained at 0.6% alkali extraction, which was possibly due to the cleavage of ester bonds between hemicelluloses and lignin in the cell wall under the alkaline medium. Similar results have been reported by Sun et al.,[18] who revealed that the alkali treatments cleaved the linkages between lignin and hemicelluloses, such as ester bonds between ferulic acid and hemicelluloses or between *p*-coumaric acid and lignin, and α-aryl ether linkages between lignin and hemicelluloses.

Table 1. Yield and Content (%) of Neutral Sugars of Lignin Fractions Obtained from Sweet Sorghum Stem

	lignin fractions[a]				
sugar	$L_{0.3}$	$L_{0.6}$	$L_{1.0}$	$L_{1.5}$	$L_{2.5}$
arabinose	0.20	0.02	0.04	0.09	0.21
galactose	0.16	0.03	0.20	0.14	0.12
glucose	0.62	0.26	0.22	0.15	0.65
xylose	0.38	0.13	0.26	0.17	1.45
total sugars[b]	1.36	0.44	0.72	0.55	2.43
yields[c]	0.8	5.2	2.3	2.4	2.0

[a] $L_{0.3}$, $L_{0.6}$, $L_{1.0}$, $L_{1.5}$, and $L_{2.5}$ represent the lignin fractions isolated by successive extractions with 0.3, 0.6, 1.0, and 1.5% KOH aqueous solution and 60% ethanol containing 2.5% KOH at 75 °C for 3 h, respectively. [b] Represents the total associated carbohydrates in the lignin fractions (% dried lignin). [c] Represents the yields of the acid-insoluble lignin fractions (% dried, dewaxed material, w/w).

To verify the purity of the extracted lignin fractions, the associated neutral sugars and uronic acids of the lignin samples were analyzed by HPAEC. As can be seen in Table 1, all the lignin fractions contained a rather low amount of associated polysaccharides (0.44−2.43%). Obviously, xylose (0.13−1.45%) and glucose (0.15−0.65%) were the major sugar constituents of the five lignin fractions, while galactose and arabinose were identified to be minor sugar constituents. However, glucuronic and galacturonic acids were not detected in all the lignin fractions in this experiment. The four lignin fractions had lower neutral sugar contents (0.44−1.36% in $L_{0.3}$−$L_{1.5}$) than the lignin extracted with alkaline ethanol solution (2.43% in $L_{2.5}$), implying that the four lignin fractions had higher purity than the lignin extracted with alkaline ethanol. $L_{0.6}$ and $L_{1.5}$ had relatively higher purities than other samples; therefore, the two fractions were used for further structural analysis.

Molecular Weight Analysis. The weight-average (M_w) and number-average (M_n) molecular weights and polydispersity (M_w/M_n) of all the lignin samples were calculated on the basis of the curves in Figure 2, and the results are listed in Table 2.

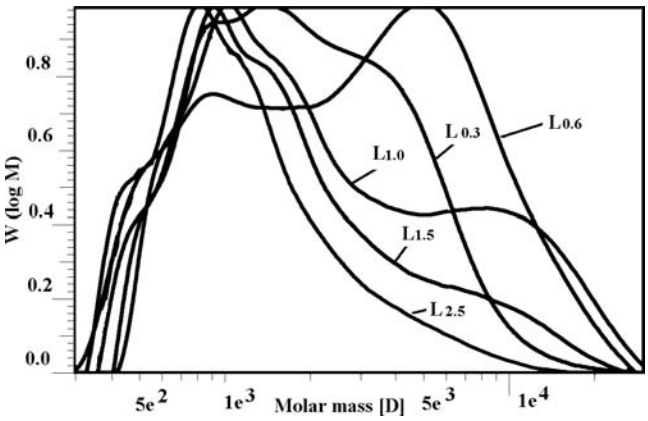

Figure 2. Molecular weight distribution curves of the five lignin fractions.

Table 2. Weight-Average (M_w) and Number-Average (M_n) Molecular Weights and Polydispersity (M_w/M_n) of Lignin Fractions Isolated from Sweet Sorghum Stem

	lignin fractions[a]				
	$L_{0.3}$	$L_{0.6}$	$L_{1.0}$	$L_{1.5}$	$L_{2.5}$
M_w	2520	3790	3910	2680	2050
M_n	1350	1530	1250	1150	1040
M_w/M_n	1.87	2.48	3.12	2.33	1.97

[a] Corresponding to the lignin fractions in Table 1.

As can be seen, the M_w and M_n of the lignin samples ranged from 2050 to 3910 g/mol and from 1040 to 1530 g/mol, respectively. Apparently, the four lignin fractions (M_w, 2520−3910 g/mol) had higher molecular weights than the lignin treated with alkaline ethanol (M_w, 2050 g/mol). The increase of the KOH concentration from 0.3 to 1.0% resulted in a notable increase of M_w from 2520 to 3910 g/mol. However, when the KOH concentration was further increased to 2.5%, the M_w value distinctly decreased to 2050 g/mol. The result was probably due to the degradation of the released lignin at a relatively high concentration of alkali. It was noted that the lignin fraction extracted with 1.0% KOH had a higher M_w than the other four lignin samples. However, the highest polydispersity of the sample suggested that the lignin fraction extracted with 1.0% KOH exhibited relatively broad molecular distributions as compared to other lignin samples. In brief, the heterogeneous molecular weights and polydispersities basically responded to gradual alkaline treatments and also indicated the inhomogeneous distributions of lignin fractions in the plant cell wall.

FT-IR Spectra Analysis. Figure 3 shows the FT-IR spectra of all the lignin fractions from sweet sorghum stem, and the bands were assigned according to the literature.[19−21] As can be seen, a prominent band at around 3451 cm^{-1} originates from the O−H stretching vibration in the aromatic and aliphatic

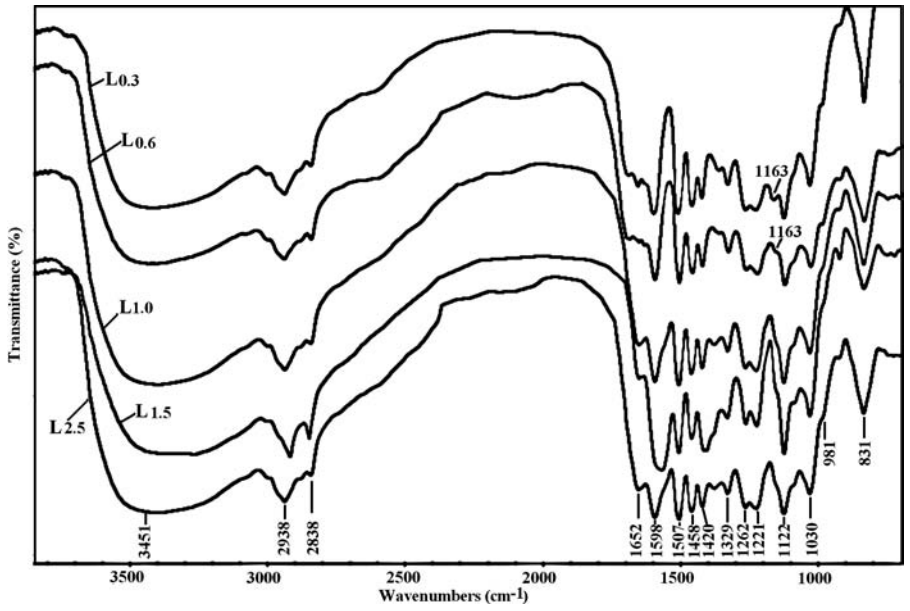

Figure 3. FT-IR spectra of the lignin fractions isolated with 0.3% ($L_{0.3}$), 0.6% ($L_{0.6}$), 1.0% ($L_{1.0}$), and 1.5% ($L_{1.5}$) KOH aqueous solution and 60% ethanol containing 2.5% ($L_{2.5}$) KOH at 75 °C for 3 h.

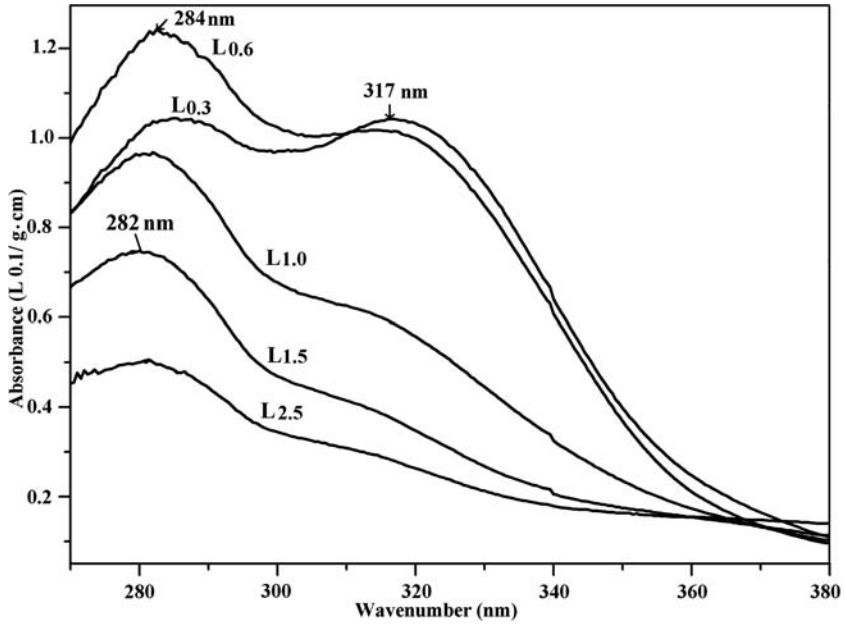

Figure 4. UV spectra of all lignin fractions ($L_{0.3}$, $L_{0.6}$, $L_{1.0}$, $L_{1.5}$, and $L_{2.5}$).

structure, and the bands at 2938 and 2838 cm^{-1} are due to a C−H vibration sketch in the CH_2 and CH_3 groups, respectively. The band at 1652 cm^{-1} is related to conjugated carbonyl stretching in the lignin fractions. The bands at 1598, 1507, and 1420 cm^{-1} are attributed to aromatic skeleton vibrations, indicating a primary structure of the lignin fractions. The band at 1458 cm^{-1}, corresponding to the C−H asymmetric vibrations and deformations (asymmetric in methyl and methylene), was also observed. The bands at 1329 cm^{-1} (syringyl ring plus guaiacyl ring condensed), 1262 cm^{-1} (guaiacyl ring breathing with C═O stretching), and 1221 cm^{-1} (ring breathing with C−C, C−O, and C═O stretching) are present. It was noted that the small band at 1163 cm^{-1} observed in the spectra of lignin fractions $L_{0.3}$ and $L_{0.6}$ was due to antisymmetric C−O stretching of ester groups. However, this band disappeared in the lignin samples $L_{1.0}$, $L_{1.5}$, and $L_{2.5}$. This fact suggested that tiny ester bands in the initial extracting lignin fractions $L_{0.3}$ and $L_{0.6}$) were retained, although most of the ester bands have been cleaved, as revealed by NMR results below. However, this band disappeared in the subsequently isolated lignin fractions $L_{1.0}$, $L_{1.5}$, and $L_{2.5}$, indicating that the ester bonds in the lignin fractions were fundamentally cleaved after alkali extraction with over 0.6% KOH in this study. Moreover, the bands of 1122 and 1030 cm^{-1} arise from the aromatic in-plane C−H bending deformation for syringyl (S) type and guaiacyl (G) type lignin units, respectively. Furthermore, the band at 981 cm^{-1} is indicative of a −HC═CH− group (out-of-plane deformation), which further confirmed that the conjugated units predominately occurred in the lignin fractions. The band at 831 cm^{-1} represents C−H

dx.doi.org/10.1021/jf400824p | J. Agric. Food Chem. 2013, 61, 4226−4235

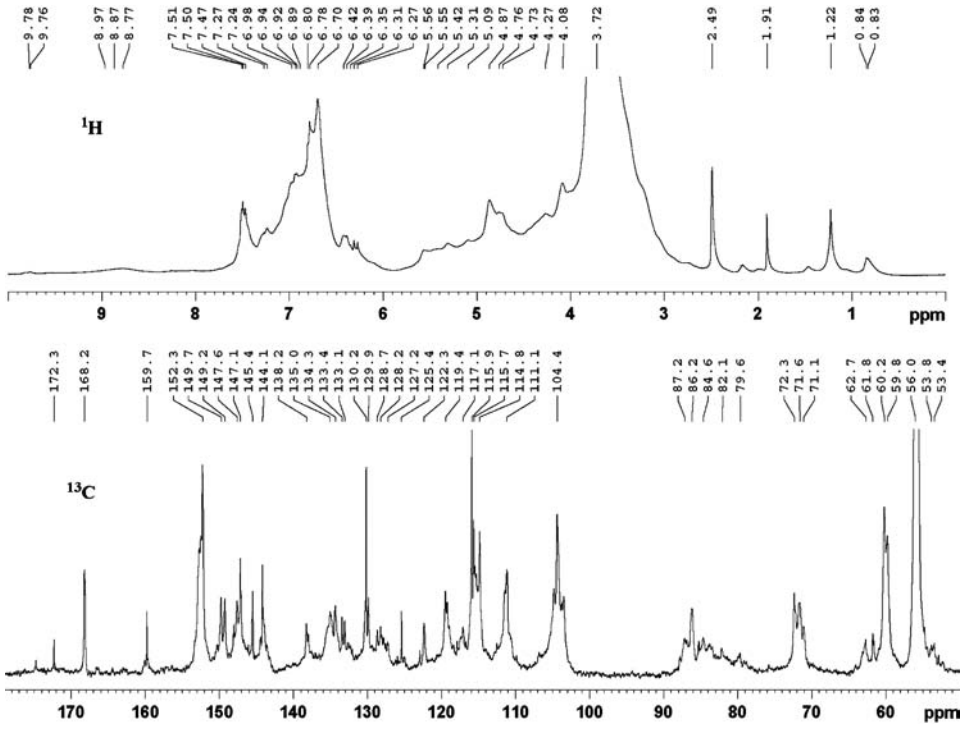

Figure 5. ^{1}H and ^{13}C NMR spectra of the lignin fraction $L_{0.6}$.

out-of-plane deformation in positions 2 and 6 of S units and all positions of *p*-hydroxyphenyl (H) units.

UV Spectral Analysis. UV spectroscopy has been used to determine the purity of lignin samples or monitor the lignin distribution among various tissues of plants with respect to the concentration.[22] Figure 4 illustrates the UV spectra of the five lignin samples, exhibiting the typical UV spectra of lignin with two maximum at 282 ($L_{1.0}$, $L_{1.5}$, and $L_{2.5}$) or 284 ($L_{0.3}$ and $L_{0.6}$) and 317 ($L_{0.3}$ and $L_{0.6}$) nm. The first maximum absorption at 282−284 nm indicated a relatively high proportion of G units in the lignin fractions. The phenomenon could be confirmed by the subsequent quantitative result based on 2D-HSQC spectra. The absorption at 317 nm, corresponding to the n → π^* transition in lignin units containing C_α═O groups and the $\pi \rightarrow \pi^*$ transition in lignin units with C_α═C_β linkages conjugated to the aromatic ring, is indicative of ferulic and *p*-coumaric acids.[23,24] As can be seen, 317 nm appeared in $L_{0.3}$ and $L_{0.6}$, whereas the absorption peak dramatically decreased in the fractions $L_{1.0}$, $L_{1.5}$, and $L_{2.5}$. This fact suggested that the linkages between *p*-coumaric/ferulic acids and lignin were significantly cleaved during the 0.6% KOH extracting procedures in this experiment, which was in agreement with the subsequent NMR analysis.

^{1}H and ^{13}C NMR Spectral Analysis. To further elucidate the structural features of the lignins extracted with aqueous alkaline solutions, the fraction $L_{0.6}$ was characterized by NMR spectroscopy. ^{1}H and ^{13}C NMR spectra of lignin fraction $L_{0.6}$ are shown in Figure 5, and the signals were assigned according to previous publications.[16,18,25]

^{1}H Spectral Analysis of Lignin. In the ^{1}H spectrum of $L_{0.6}$, signals between 6.00 and 8.00 ppm could be ascribed to aromatic protons in S, G, and H units as well as *p*-coumaric acid (PCA) and ferulic acid (FA). More specifically, an intense signal at 2.49 ppm is indicative of residual protons in DMSO-d_6. The signals at 7.51, 7.50, 6.80, and 6.31 ppm are attributed to $H_{2/6}$, H_7, $H_{3/5}$, and H_8 of PCA, respectively. Meanwhile, the signals at 7.27, 7.50, and 6.42 ppm originate from H_2, H_7, and H_8 of FA, respectively. Moreover, the signals at 6.98 and 6.78 ppm, 6.70 ppm, and 7.19 ppm are related to the aromatic protons in G, S, and H units, respectively. Furthermore, the H_α in *α,β*-diaryl ether showed a signal at 5.56 ppm, whereas a weak peak at 5.55 ppm could be attributed to phenylcoumaran structures in this lignin fraction. The H_γ in *p*-hydroxycinnamyl alcohol end groups showed a signal at 4.08 ppm. Signals at 4.87 and 3.72 ppm arise from H_α in the *β-O*-4′ structure and methoxyl protons ($-OCH_3$), respectively. Protons in aliphatic groups exhibited signals between 0.80 and 1.50 ppm. Protons in methyl ($-CH_3$) and methylene ($-CH_2$) in saturated aliphatic side chains of lignin showed signals at 0.84 and 1.22 ppm.

^{13}C Spectral Analysis of Lignin. As can be seen, the ^{13}C NMR spectrum of $L_{0.6}$ is almost absent of typical polysaccharide signals between 57.0 and 103.0 ppm, implying that the lignin sample contained small amounts of associated polysaccharides, which corresponded to the results of sugar analysis. The region between 104.4 and 168.2 ppm represents the aromatic region of the lignin. The S units give signals at 152.3 ppm (C-3/C-5, etherified), 147.1 ppm (C-3/C-5, nonetherified), 138.2 ppm (C-4, etherified), 134.3 ppm (C-1, etherified), 106.8 (C-2/C-6, oxidized), and 104.4 ppm (C-2/C-6). The G units were found at 149.7 ppm (C-3, etherified), 145.4 ppm (C-4, nonetherified), 134.3 ppm (C-1, etherified), 133.1 ppm (C-1, nonetherified), 119.4 ppm (C-6, nonetherified), 114.8 ppm (C-5, nonetherified), and 111.1 ppm (C-2, nonetherified). The H units were identified at 127.2 ppm (C-2/C-6). The signals aforementioned revealed that the lignin fraction belonged to the typical grass lignin, in accordance with the FT-IR analysis. Moreover, other characteristic signals in the ^{13}C NMR spectrum exhibited six strong resonances at 168.2, 159.7, 144.1, 130.2, 125.4, 115.9, and 115.7 ppm, corresponding to C-9 (*γ*), C-4, C-7 (*a*), C-2/C-6, C-1, C-3/C-5, and C-8

dx.doi.org/10.1021/jf400824p | J. Agric. Food Chem. 2013, 61, 4226−4235

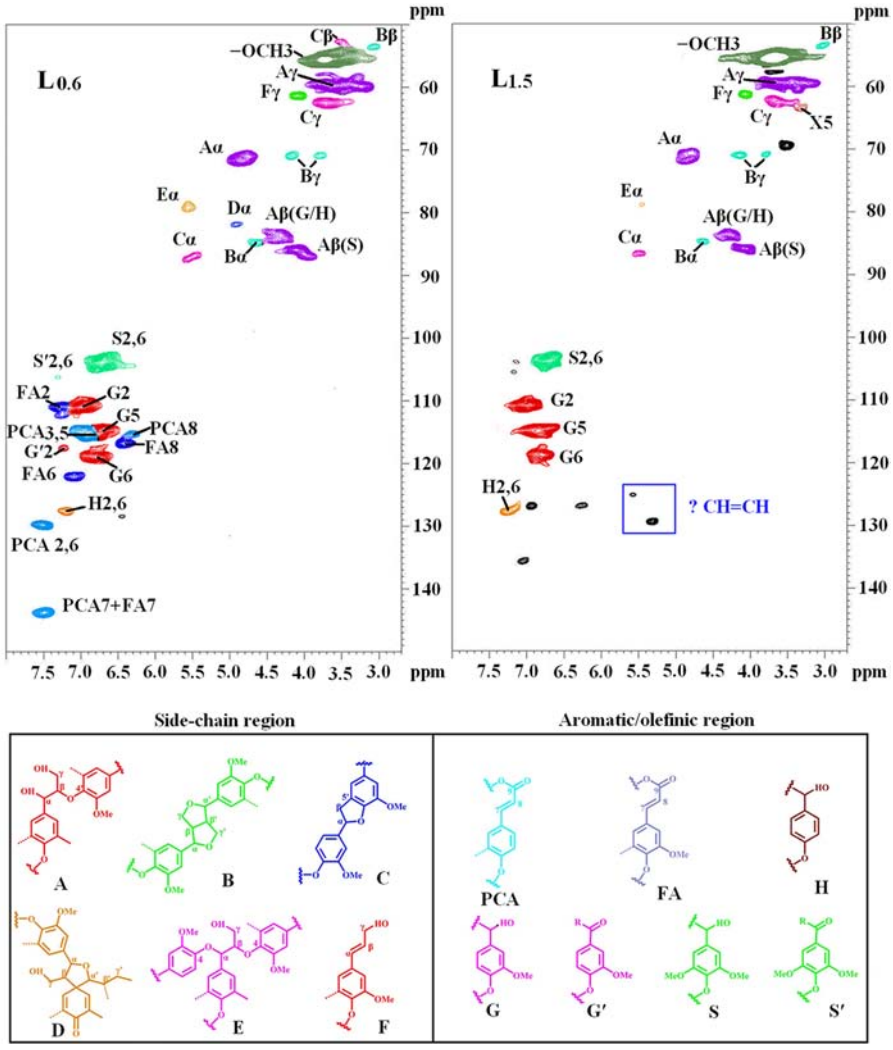

Figure 6. HSQC spectra of the lignin fractions $L_{0.6}$ and $L_{1.5}$ and their main structures present in sweet sorghum lignin fraction $L_{0.6}$: (A) *β*-aryl-ether units (*β*-*O*-4′); (B) resinol substructures (*β*-*β*′); (C) phenylcoumaran substructures (*β*-5′); (D) spirodienones (*β*-1′); (E) *α*,*β*-diaryl ethers (*α*-*O*-4/*β*-*O*-4); (F) *p*-hydroxycinnamyl alcohol end groups; (PCA) *p*-coumaric acid; (FA) ferulic acid; (H) *p*-hydroxyphenyl units; (G) guaiacyl units; (G′) oxidized guaiacyl units with a C_α ketone; (S) syringyl units; (S′) oxidized syringyl units bearing a carbonyl at C_α.

(*β*) in PCA, respectively, while FA shows signals at 168.2, 144.1, and 122.3 ppm, corresponding to C-9 (*γ*), C-7 (*a*), and C-6. The signal of C-9 (*γ*) in esterified PCA was tiny but could be observed at 166.5 ppm. The etherified FA C-6 was found with a weak signal at 123.0 ppm (data not shown). These facts suggested that PCA was linked to lignin by ester bonds, which were easily cleaved during alkali treatment at the condition given, whereas FA was mostly linked to lignin by ether bonds. Additionally, signals between 50 and 86 ppm are attributed to lignin interunit linkages in the ^{13}C NMR spectrum. Especially, the *β*-*O*-4′ linkages were observed by signals at 86.2 (S units)/84.6 (G and H units), 72.3, and 60.2 ppm, assigned to C-*β*, C-*a*, and C-*γ*, respectively. A strong signal at about 56.0 ppm was ascribed to $-OCH_3$ groups in G and S units.

2D-HSQC NMR Spectral Analysis. **2D-HSQC NMR Spectra.** 2D-HSQC spectroscopy is a powerful tool for determination of lignin structures. To further illustrate the structural features of lignins, the fractions $L_{0.6}$ and $L_{1.5}$ were investigated by 2D-HSQC NMR spectra. In terms of the structures of the two lignin samples $L_{0.6}$ and $L_{1.5}$, the side-chain (aliphatic-oxygenated, around δ_C/δ_H 50.0−90.0/2.50−6.00) and aromatic/olefinic (around δ_C/δ_H 100.0−150.0/5.50−8.50) regions of the HSQC spectra are illustrated in Figure 6. The assignments of primary lignin correlated signals in the HSQC spectra are listed in Table 3, and the main substructures are represented in Figure 6.[1,25−34]

In the lignin side-chain region, cross-signals of methoxyl groups ($-OCH_3$, δ_C/δ_H 55.8/3.72) and the different interunit linkages of sweet sorghum stem lignin were detected. The lignin is rich in *β*-ether (*β*-*O*-4′) (A), with small amounts of resinol (*β*-*β*′) (B) and phenylcoumaran (*β*-5′) (C). Specifically, the $C_\alpha-H_\alpha$ correlations in *β*-*O*-4′ substructures linked to G units were observed at δ_C/δ_H 71.7/4.85, whereas the $C_\gamma-H_\gamma$ correlations in *β*-*O*-4′ substructures were located at δ_C/δ_H 59.8/3.62. The $C_\beta-H_\beta$ correlations at δ_C/δ_H 84.0/4.28 and 86.0/4.11 linked to G/H units and S lignin units in *β*-*O*-4′ substructures, respectively. Moreover, resinol (*β*-*β*′) substructures with strong signals were also observed in the HSQC spectra. The signals were detected with their $C_\alpha-H_\alpha$, $C_\beta-H_\beta$, and double $C_\gamma-H_\gamma$ correlations at δ_C/δ_H 84.8/4.65, 53.6/3.06, and 71.0/4.17 and 3.79, respectively. Phenylcoumaran (*β*-5′) substructures were also detected, and the signals for their $C_\alpha-H_\alpha$, $C_\beta-H_\beta$, and $C_\gamma-H_\gamma$ correlations were observed at δ_C/δ_H 87.2/5.52, 52.7/3.51, and 62.5/3.71, respectively. The two

dx.doi.org/10.1021/jf400824p | J. Agric. Food Chem. 2013, 61, 4226−4235

Table 3. Assignments of $^{13}C-^{1}H$ Cross-Signals in HSQC Spectra of Alkali-Extractable Lignin Fraction $L_{0.6}$ from Sweet Sorghum Stem[a]

label	δ_C/δ_H (ppm)	assignments
C_β	52.7/3.51	$C_\beta-H_\beta$ in phenylcoumaran substructures (C)
B_β	53.6/3.06	$C_\beta-H_\beta$ in β-β' (resinol) substructures (B)
$-OCH_3$	55.8/3.72	C−H in methoxyls
A_γ	59.8/3.62	$C_\gamma-H_\gamma$ in β-O-4′ substructures (A)
F_γ	61.4/4.08	$C_\gamma-H_\gamma$ in p-hydroxycinnamyl alcohol end groups (F)
C_γ	62.5/3.71	$C_\gamma-H_\gamma$ in phenylcoumaran substructures (C)
B_γ	71.0/3.79−4.17	$C_\gamma-H_\gamma$ in β-β' resinol substructures (B)
$A_{\alpha(S)}$	71.7/4.85	$C_\alpha-H_\alpha$ in β-O-4′ linked to an S unit (A)
E_α	79.2/5.56	$C_\alpha-H_\alpha$ in α,β-diaryl ethers (E)
D_α	81.9/4.91	$C_\alpha-H_\alpha$ in spirodienone substructures (D)
$A_{\beta(G/H)}$	84.0/4.28	$C_\beta-H_\beta$ in β-O-4′ linked to a G/H unit (A)
B_α	84.8/4.65	$C_\alpha-H_\alpha$ in β-β' resinol substructures (B)
$A_{\beta(S)}$	86.0/4.11	$C_\beta-H_\beta$ in β-O-4′ linked to an S unit (A)
C_α	87.2/5.52	$C_\alpha-H_\alpha$ in phenylcoumaran substructures (C)
$S_{2,6}$	104.0/6.71	$C_{2,6}-H_{2,6}$ in syringyl units (S)
$S'_{2,6}$	106.3/7.31	$C_{2,6}-H_{2,6}$ in oxidized S units (S′)
G_2	110.9/6.98	C_2-H_2 in guaiacyl units (G)
G'_2	118.1/7.25	C_2-H_2 in oxidized G units (G′)
G_5	114.7/6.70	C_5-H_5 in guaiacyl units (G)
G_6	119.1/6.78	C_6-H_6 in guaiacyl units (G)
$H_{2,6}$	127.6/7.19	$C_{2,6}-H_{2,6}$ in H units (H)
$PCA_{3,5}$	115.4/6.79	$C_{3,5}-H_{3,5}$ in p-coumaric acid (PCA)
$PCA_{2,6}$	129.8/7.51	$C_{2,6}-H_{2,6}$ in p-coumaric acid (PCA)
PCA_7	143.8/7.49	C_7-H_7 in p-coumaric acid (PCA)
PCA_8	115.4/6.30	C_8-H_8 in p-coumaric acid (PCA)
FA_2	110.0/7.28	C_2-H_2 in ferulic acid (FA)
FA_6	122.7/7.11	C_6-H_6 in ferulic acid (FA)
FA_7	143.8/7.49	C_7-H_7 in ferulic acid (FA)
FA_8	116.8/6.41	C_8-H_8 in ferulic acid (FA)

[a]Signals were assigned by comparison with the literature.[1,25−34]

signals corresponding to the $C_\alpha-H_\alpha$ correlations of spirodienone substructures (D) and α,β-diaryl ethers (E) were detected at δ_C/δ_H 81.9/4.91 and 79.2/5.56, respectively. In addition, p-hydroxycinnamyl alcohol end groups (F) were recognized by $C_\gamma-H_\gamma$ correlations at δ_C/δ_H 61.4/4.08.

In the aromatic regions/olefinic regions, cross-signals from S, G, and H units were observed. The S units showed a prominent signal for a $C_{2,6}-H_{2,6}$ correlation at δ_C/δ_H 104.0/6.71. The G units exhibited different correlations for C_2-H_2 (δ_C/δ_H 110.9/6.98), C_5-H_5 (δ_C/δ_H 114.7/6.70), and C_6-H_6 (δ_C/δ_H 119.1/6.78), respectively. The $C_{2,6}-H_{2,6}$ aromatic correlation signals from H units were explicitly observed at δ_C/δ_H 127.6/7.19. In addition, the C_α-oxidized S units (S′) exhibited a correlation for $C_{2,6}-H_{2,6}$ (δ_C/δ_H 106.3/7.31), and oxidized guaiacyl units with a C_α ketone (G′) showed a correlation for C_2-H_2 (δ_C/δ_H 118.1/7.25) in the HSQC spectrum of $L_{0.6}$. However, no signals of S′ and G′ were detected in $L_{1.5}$ (in the current contour level), implying that $L_{0.6}$ had higher oxidized units than $L_{1.5}$.

Furthermore, in terms of the HSQC spectrum of the lignin fraction $L_{0.6}$, the dissociated PCA_8 (C_8-H_8) correlations are located at δ_C/δ_H 115.4/6.30. The cross-signals corresponding to correlations $C_{2,6}-H_{2,6}$, $C_{3,5}-H_{3,5}$, and C_7-H_7 in dissociated PCA were observed at δ_C/δ_H 129.8/7.51, 115.4/6.79, and 143.8/7.49, respectively. It was noted that a small amount of esterified PCA was observed in fraction $L_{0.6}$ (not shown in current contour level). Likewise, the FA_8 (C_8-H_8) correlation at δ_C/δ_H 116.8/6.41 suggested ester linkages occurring at the 9-positions of FA, which are linked to C-5 of arabinose in araboxylans, were mostly cleaved in the lignin preparations (as revealed by a lower content of associated sugars in $L_{0.6}$), whereas the ether bonds linked to lignin side-chain by phenolic hydroxyl groups probably remained intact under the conditions used.[25] In addition, the FA_7 (C_7-H_7) correlation coincides with that of PCA_7 at δ_C/δ_H 143.8/7.49, while its C_2-H_2 and C_6-H_6 correlations appeared at δ_C/δ_H 110.0/7.28 and 122.7/7.11, respectively. As compared to $L_{0.6}$, the signals for PCA and FA were not found in the HSQC spectrum of $L_{1.5}$. The above-mentioned fact indicated that PCA and FA were released and co-precipitated in the lignin fractions isolated from the initial extracting steps ($L_{0.3}$ and $L_{0.6}$); however, these hydroxycinnamic acids (PCA and FA) were not detected in the lignin fractions extracted in the subsequent procedures ($L_{1.0}$, $L_{1.5}$, and $L_{2.5}$), which is consistent with the results of FT-IR and UV spectral analyses. Some additional signals appearing at δ_C/δ_H 125.1/5.57 and 129.5/5.31 in $L_{1.5}$ were probably due to the occurrence of olefinic (C═C) structures in lignin, which still needs further confirmation (Figure 6).[31] To sum up, 2D-HSQC NMR spectra suggested that the lignin isolated by successive alkali extractions has inhomogeneous structural features.

Semiquantitative 2D-HSQC Spectra. According to the semiquantitative methods in the literature,[1,29] the relative amounts of interunit linkages and S/G molar ratios present in $L_{0.6}$ and $L_{1.5}$ were calculated as shown in Table 4. As expected,

Table 4. Quantitative Characteristics of Lignin Fractions $L_{0.6}$ and $L_{1.5}$ from Quantitative 2D-HSQC Spectral Method

	$L_{0.6}$[a]	$L_{1.5}$[a]
β-aryl-ether units (β-O-4′, A)	76.0[b]	68.8
resinol substructures (β-β', B)	7.4	13.2
phenylcoumaran substructures (β-5′,C)	8.7	13.0
spirodienones (β-1′, D)	2.0	ND[e]
α,β-diaryl ethers (α-O-4/β-O-4, E)	5.9	5.0
PCA/FA ratio[c]	1.0	ND
S/G/H ratio[d]	47/50/3	37/62/1

[a]Corresponding to the lignin fractions in Table 1. [b]Relative quantitative method based on 2D-HSQC spectra (without IS). [c]PCA/FA ratio obtained by the following equation: PCA/FA ratio = $0.5I_{PCA_{2,6}}/I_{FA_2}$. [d]S/G/H ratio obtained by the following equation: S/G/H ratio = $0.5I_{S_{2,6}}/I_{G_2}/0.5I_{H_{2,6}}$. [e]Not detected in the current contour level.

the main lignin substructures were β-O-4′ aryl ether (over 68.0% of total side chains), followed by low amounts of resinol (β-β'), phenylcoumaran (β-5′), spirodienones (β-1′), and α,β-diaryl ethers (α-O-4/β-O-4). Specifically, the abundance of β-O-4′ aryl ether in $L_{0.6}$ (76.0%) was higher than that in $L_{1.5}$ (68.8%), which was probably related to the degradation of the released lignin at a relatively high concentration of alkali. In addition, $L_{0.6}$ contained lower amounts of spirodienone substructures (2.0%), whereas this substructure was not detected in $L_{1.5}$ in the current contour level. The difference might be attributed to the different concentrations of alkaline aqueous solutions used for extracting the lignin fractions. The ratio of S/G/H was estimated to be 47/50/3 for $L_{0.6}$ and 37/62/1 for $L_{1.5}$, respectively. It was thus concluded that the alkaline lignin from sweet sorghum stem was an HGS-type lignin, which had predominant amounts of G and S units

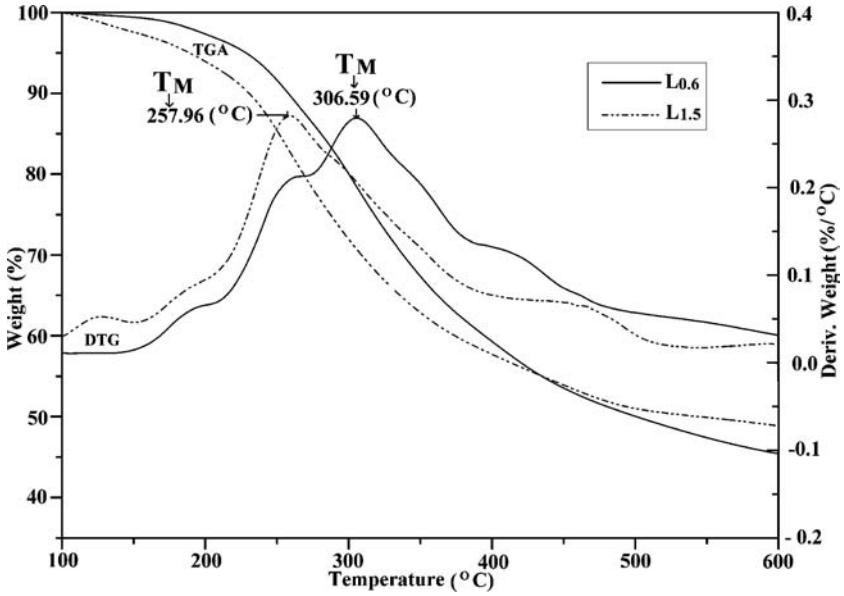

Figure 7. Thermogram of the lignin fractions $L_{0.6}$ and $L_{1.5}$.

together with a minor proportion of H units. The ratio of S/G/H also suggested that the S-rich lignin fraction was more easily released than the G-rich lignin in the initial process under the present investigation, in line with recent literature.[10] This fact is also in agreement with a recent publication in which the authors have stated that the higher content of syringyl units resulted in the easy delignification under alkaline conditions.[32] In addition, the higher G units in the subsequently extracted lignin fraction ($L_{1.5}$) also suggested that the G-rich lignin fraction was probably released in the later extracting procedures under the successive alkali extractions. However, the finding is different from a recent study in which the authors found that lignin fragments with lower S/G ratios were initially extracted by acetone after ionic liquid ([C2 min][OAc]) pretreatments, whereas the lignin subsequently extracted with dioxane is rich in S units.[33] The differences probably depend on the diverse reagents and reaction mediums used in the respective experiment, which also potentially revealed the effects of targeted selectivity of reagents and reaction mediums on the inhomogeneous lignin macromolecules. In addition, the differences in the ratios of PCA/FA and S/G/H among the lignin fractions were probably caused by the specific fractionation process. Furthermore, it was also observed that $L_{1.5}$ had a higher proportion of carbon−carbon (C−C) structures (26.2%) than $L_{0.6}$ (18.1%), which was probably due to the higher content of G units in the lignin fraction.[34]

Thermal Analysis. To study the relationship between structure features and thermal properties, the TGAs of $L_{0.6}$ and $L_{1.5}$ were comparatively investigated (Figure 7). The maximum decomposition temperature (T_{max}) was defined in a previous study;[35] and it is the corresponding temperature of the maximum decomposition rate (V_{max}). As shown in Figure 7, it was found that the T_{max} of $L_{1.5}$ (~258 °C) was less than that of $L_{0.6}$ (~307 °C) at the beginning of lignin decomposition (200−400 °C), which was found to be related to the molecular weight, as also revealed by Sun et al.[9] In a word, the higher molecular weights of lignins could result in a relatively higher thermal stability. This is probably because the initial reaction involves the deformation of the weaker C−O bond in the *β*-*O*-4′ structure during lignin decomposition.[36] Most of the ether bonds were expected to be cleaved at the stage of 200−400 °C,[36] confirmed by the high content of *β*-*O*-4′ in the $L_{0.6}$ fraction (Table 4). In addition, it was observed that the "char residues" at 600 °C were 44% for $L_{1.5}$ and 48% for $L_{0.6}$, respectively. This fact suggested that the high content of the residues was probably due to the higher proportion of C−C structures in the lignin (Table 4), in agreement with a recent publication.[33] From the above observations, it can be concluded that lignin with a higher molecular weight and more *β*-*O*-4′ structures has a higher T_{max} at the main lignin decomposition step. Moreover, lignin having more C−C structures potentially led to more "char residue". In other words, the different thermal properties of the lignin fractions suggested that the lignins isolated by successive alkali extractions have inhomogeneous structural features under the present investigation.

To conclude, in the successive KOH extraction processes, a total yield of the five lignin fractions accounting for 80.3% of the original lignin from the cell walls of sweet sorghum stem was extracted. This fact suggested that the successive alkali treatment was an effective process to extract lignin with inhomogeneous chemical and structural features. The alkali lignin fractions from sweet sorghum stem are typical grass lignin with a dominating content of G units. The lignin fractions are mostly composed of *β*-*O*-4′ aryl ether linkages, together with lower amounts of *β*-*β*′, *β*-5′, *β*-1′, and *α*,*β*-diaryl ethers linkages. In addition, hydroxycinnamic acids (mainly *p*-coumaric acid) attached to lignin were released and co-precipitated in the lignin fractions isolated in the initial extracting steps, whereas hydroxycinnamic acids (*p*-coumaric and ferulic acids) were not detected in the subsequently extracted lignin fractions. The higher proportion of C−C structures was probably related to the higher G units in the lignin, as revealed by HSQC spectra. Furthermore, the data obtained also showed that thermal stability is positively related to the molecular weights, while a higher content of C−C structures in the lignin fractions potentially led to a higher "char residue" after thermal decomposition at 600 °C. Thus, lignin molecules extracted from successive KOH extraction processes could be used in revealing the inhomogeneous chemical features of the lignin in a herbaceous plant.

AUTHOR INFORMATION

Corresponding Author

*Phone: +86-10-62336903. Fax: +86-10-62336903. E-mail: rcsun3@bjfu.edu.cn.

Funding

The authors are extremely grateful for financial support from National Natural Science Foundation of China (31110103902), Major State Basic Research Projects of China (973-2010CB732204), and State Forestry Administration (201204803).

Notes

The authors declare no competing financial interest.

REFERENCES

(1) Martínez, Á. T.; Rencoret, J.; Marques, G.; Gutiérrez, A.; Ibarra, D.; Jiménez-Barbero, J.; del Río, J. C. Monolignol acylation and lignin structure in some nonwoody plants: a 2D NMR study. *Phytochemistry* **2008**, *69*, 2831−2843.

(2) Boerjan, W.; Ralph, J.; Baucher, M. Lignin biosynthesis. *Annu. Rev. Plant Biol.* **2003**, *54*, 519−546.

(3) Ralph, J.; Lundquist, K.; Brunow, G.; Lu, F.; Kim, H.; Schatz, P. F.; Marita, J. M.; Hatfield, R. D.; Ralph, S. A.; Christensen, J. H. Lignins: natural polymers from oxidative coupling of 4-hydroxyphenyl-propanoids. *Phytochem. Rev.* **2004**, *3*, 29−60.

(4) Çetin, N. S.; Özmen, N. Use of organosolv lignin in phenol-formaldehyde resins for particleboard production: II. Particleboard production and properties. *Int. J. Adhes. Adhes.* **2002**, *22*, 481−486.

(5) Sun, R. C. Detoxification and separation of lignocellulosic biomass prior to fermentation for bioethanol production by removal of lignin and hemicelluloses. *Bioresources* **2009**, *4*, 452−455.

(6) Li, M. F.; Sun, S. N.; Xu, F.; Sun, R. C. Microwave-assisted organic acid extraction of lignin from bamboo: structure and antioxidant activity investigation. *Food Chem.* **2012**, *134*, 1392−1398.

(7) Faustino, H.; Gil, N.; Baptista, C.; Duarte, A. P. Antioxidant activity of lignin phenolic compounds extracted from kraft and sulphite black liquors. *Molecules* **2010**, *15*, 9308−9322.

(8) Pan, X.; Kadla, J. F.; Ehara, K.; Gilkes, N.; Saddler, J. N. Organosolv ethanol lignin from hybrid poplar as a radical scavenger: relationship between lignin structure, extraction conditions, and antioxidant activity. *J. Agric. Food Chem.* **2006**, *54*, 5806−5813.

(9) Sun, R. C.; Tomkinson, J.; Lloyd Jones, G. Fractional characterization of ash-AQ lignin by successive extraction with organic solvents from oil palm EFB fibre. *Polym. Degrad. Stab.* **2000**, *68*, 111−119.

(10) Sun, S. N.; Li, M. F.; Yuan, T. Q.; Xu, F.; Sun, R. C. Sequential extractions and structural characterization of lignin with ethanol and alkali from bamboo (*Neosinocalamus affinis*). *Ind. Crops Prod.* **2012**, *37*, 51−60.

(11) Xiao, L.; Xu, F.; Sun, R. C. Chemical and structural characterization of lignins isolated from *Caragana sinica*. *Fiber Polym.* **2011**, *12*, 316−323.

(12) Billa, E.; Koullas, D. P.; Monties, B.; Koukios, E. G. Structure and composition of sweet sorghum stalk components. *Ind. Crops Prod.* **1997**, *6*, 297−302.

(13) Gnansounou, E.; Dauriat, A.; Wyman, C. Refining sweet sorghum to ethanol and sugar: economic trade-offs in the context of north China. *Bioresour. Technol.* **2005**, *96*, 985−1002.

(14) Mohanty, A.; Misra, M.; Drzal, L. Sustainable bio-composites from renewable resources: opportunities and challenges in the green materials world. *J. Polym. Environ.* **2002**, *10*, 19−26.

(15) Liu, W.; Budtova, T.; Navard, P. Influence of ZnO on the properties of dilute and semi-dilute cellulose-NaOH-water solutions. *Cellulose* **2011**, *18*, 911−920.

(16) She, D.; Xu, F.; Geng, Z. C.; Sun, R. C.; Jones, G. L.; Baird, M. S. Physicochemical characterization of extracted lignin from sweet sorghum stem. *Ind. Crops Prod.* **2010**, *32*, 21−28.

(17) Sluiter, A.; Hames, B.; Ruiz, R.; Scarlata, C.; Sluiter, J.; Templeton, D.; Crocker, D. Determination of structural carbohydrates and lignin in biomass. Laboratory Analytical Procedure, technical report NREL/TP-510-42618, 2008.

(18) Sun, X. F.; Sun, R.; Fowler, P.; Baird, M. S. Extraction and characterization of original lignin and hemicelluloses from wheat straw. *J. Agric. Food Chem.* **2005**, *53*, 860−870.

(19) Faix, O. Classification of lignins from different botanical origins by FT-IR spectroscopy. *Holzforschung* **1991**, *45*, 21−27.

(20) Faix, O. Fourier transform infrared spectroscopy. In *Methods in Lignin Chemistry*; Lin, S. Y., Dence, C. W., Eds.; Springer-Verlag: Berlin, 1992; pp 83−109.

(21) Faix, O. Classification of lignins from different botanical origins by FT-IR spectroscopy. *Holzforschung* **2009**, *45*, 21−28.

(22) Sun, R. C.; Lu, Q.; Sun, X. Physico-chemical and thermal characterization of lignins from *Caligonum monogoliacum* and *Tamarix* spp. *Polym. Degrad. Stab.* **2001**, *72*, 229−238.

(23) Oliveira, L.; Evtuguin, D.; Cordeiro, N.; Silvestre, A. Structural characterization of stalk lignin from banana plant. *Ind. Crops Prod.* **2009**, *29*, 86−95.

(24) Sun, J. X.; Sun, X. F.; Sun, R. C.; Fowler, P.; Baird, M. S. Inhomogeneities in the chemical structure of sugarcane bagasse lignin. *J. Agric. Food Chem.* **2003**, *51*, 6719−6725.

(25) Wen, J. L.; Xue, B. L.; Xu, F.; Sun, R. C.; Pinkert, A. Unmasking the structural features and property of lignin from bamboo. *Ind. Crops Prod.* **2013**, *42*, 332−343.

(26) Ralph, J.; Marita, J. M.; Ralph, S. A.; Hatfield, R. D.; Lu, F.; Ede, R. M.; Peng, J.; Quideau, S.; Helm, R. F.; Grabber, H. H.; Kim, H.; Jimenez-Monteon, G.; Zhang, Y.; Jung, H.-J. G.; Landucci, L. L.; MacKay, J. J.; Sederoff, R. R.; Chapple, C.; Boudet, A. M. In *Advances in Lignocellulosics Characterization*; Argyropoulos, D. S., Ed.; Tappi Press: Atlanta, GA, 1999; pp 55−108.

(27) Ralph, J.; Bunzel, M.; Marita, J. M.; Hatfield, R. D.; Lu, F.; Kim, H.; Schatz, P. F.; Grabber, J. H.; Steinhart, H. Peroxidase-dependent cross-linking reactions of phydroxycinnamates in plant cell walls. *Phytochem. Rev.* **2004**, *3*, 79−96.

(28) Ralph, S. A.; Ralph, J.; Landucci, L. L. NMR database of lignin and cell wall model compounds. Available online: http://ars.usda.gov/Services/docs.htm?docid=10491 (accessed on March 5, 2013).

(29) Wen, J. L.; Sun, S. L.; Xue, B. L.; Sun, R. C. Recent advances in characterization of lignin polymer by solution-state nuclear magnetic resonance (NMR) methodology. *Materials* **2013**, *6*, 359−391.

(30) Del Río, J. C.; Rencoret, J.; Marques, G.; Li, J.; Gellerstedt, G.; Jiménez-Barbero, J.; Martínez, A. T.; Gutiérrez, A. Structural characterization of the lignin from jute (*Corchorus capsularis*) fibers. *J. Agric. Food Chem.* **2009**, *57*, 10271−10281.

(31) Rencoret, J.; Gutiérrez, A.; Nieto, L.; Jiménez-Barbero, J.; Faulds, C. B.; Kim, H.; Ralph, J.; Martínez, Á.; del Río, J. Lignin composition and structure in young versus adult *Eucalyptus globulus* plants. *Plant Physiol.* **2011**, *155*, 667−682.

(32) Shimizu, S.; Yokoyama, T.; Akiyama, T.; Matsumoto, Y. Reactivity of lignin with different composition of aromatic syringyl/guaiacyl structures and *erythro/threo* side chain structures in *β-O*-4 type during alkaline delignification: as a basis for the different degradability of hardwood and softwood lignin. *J. Agric. Food Chem.* **2012**, *60*, 6471−6476.

(33) Wen, J. L.; Sun, S. L.; Xue, B. L.; Sun, R. C. Quantitative structures and thermal properties of birch lignins after ionic liquid pretreatment. *J. Agric. Food Chem.* **2013**, *61*, 635−645.

(34) Wang, K.; Bauer, S.; Sun, R. C. Structural transformation of *Miscanthus* × *giganteus* lignin fractionated under mild formosolv, basic organosolv, and cellulolytic enzyme conditions. *J. Agric. Food Chem.* **2012**, *60*, 144−152.

(35) Hodgson, E.; Nowakowski, D.; Shield, I.; Riche, A.; Bridgwater, A. V.; Clifton-Brown, J. C.; Donnison, I. S. Variation in *miscanthus* chemical composition and implications for conversion by pyrolysis and thermo-chemical biorefining for fuels and chemicals. *Bioresour. Technol.* **2011**, *102*, 3411−3418.

(36) Faravelli, T.; Frassoldati, A.; Migliavacca, G.; Ranzi, E. Detailed kinetic modeling of the thermal degradation of lignins. *Biomass Bioenerg.* **2010**, *34*, 290−301.